



CHORUS

This is the accepted manuscript made available via CHORUS. The article has been published as:

Probing the Topological Exciton Condensate via Coulomb Drag

M. P. Mink, H. T. C. Stoof, R. A. Duine, Marco Polini, and G. Vignale

Phys. Rev. Lett. **108**, 186402 — Published 1 May 2012

DOI: [10.1103/PhysRevLett.108.186402](https://doi.org/10.1103/PhysRevLett.108.186402)

Probing the topological exciton condensate via Coulomb drag

M. P. Mink,* H. T. C. Stoof, and R. A. Duine
*Institute for Theoretical Physics, Utrecht University,
 Leuvenlaan 4, 3584 CE Utrecht, The Netherlands*

Marco Polini
NEST, Istituto Nanoscienze-CNR and Scuola Normale Superiore, I-56126 Pisa, Italy

G. Vignale
Department of Physics and Astronomy, University of Missouri, Columbia, Missouri 65211, USA

The onset of exciton condensation in a topological insulator thin film was recently predicted. We calculate the critical temperature for this transition, taking into account screening effects. Furthermore, we show that the proximity to this transition can be probed by measuring the Coulomb drag resistivity between the surfaces of the thin film as a function of temperature. This resistivity shows an upturn upon approaching the exciton-condensed state.

Introduction. — Recently, there has been great experimental and theoretical interest in a new class of materials called topological insulators (TIs) [1]. These materials combine, for a particular doping level, an insulating behavior in the bulk with topologically protected conducting surface states that are described by a two-dimensional (2D) Dirac-Weyl Hamiltonian. When the surfaces of a TI film are independently doped or gated, electrons can be induced in one layer and holes in the other. In 2009, Seradjeh *et al.* [2] predicted that such a system can support a so-called topological exciton condensate. Electrons in one layer combine with holes in the other layer to form excitons, which condense for low enough temperatures. One of the interesting features of this state is that it supports vortices in the order parameter: these vortices carry a fractional charge $\pm e/2$ [2].

In a drag experiment with a two-layer system a current is applied through one of the layers (the drive or active layer) and an induced voltage is measured in the other layer (the passive layer). The drag resistivity ρ_D is defined as the ratio between the electric field in the passive layer and the current density in the active layer. In the absence of an ordered state, the low-temperature behavior of the drag resistivity is $\rho_D \propto T^2$ [or $T^2 \log(T)$ for a 2D system with short-range interactions]. This quadratic temperature dependence was first observed in 1991 by Gramila *et al.* [3] and is a hall mark of Fermi-liquid behavior. A review of drag effects in two-layer systems is given in Ref. [4]. A departure from the standard $\rho_D \propto T^2$ temperature dependence indicates the occurrence of non-Fermi-liquid behavior. The low-temperature dependence of ρ_D for semiconductor electron-hole bilayers was studied experimentally in numerous recent works [5, 6]. On the theoretical side, we note the calculation by Hu [7], which predicted an enhancement of Coulomb drag for ordinary electron-hole bilayers at temperatures just above the excitonic instability, and the analysis of Ref. [8],

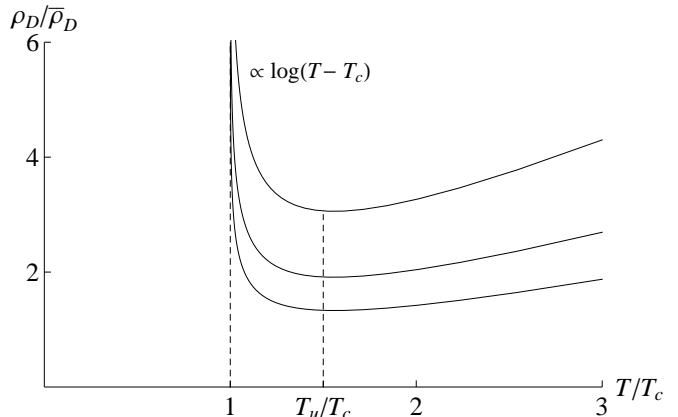


FIG. 1: The drag resistivity ρ_D [in units of $\bar{\rho}_D = (\nu_0 U)^2 \hbar/e^2$, with ν_0 the density of states at the Fermi level and U the interlayer interaction strength] calculated from Eq. (3) as a function of the reduced temperature T/T_c . With this choice of units $\rho_D/\bar{\rho}_D$ depends on two parameters – the chemical potential μ and the critical temperature T_c – which implicitly determine the interaction strength U in Eq. (1). The curves correspond to the case of equal chemical potentials in the two layers ($\mu = 0.04$ eV). From top to bottom the critical temperatures are $T_c/T_F = (1/150, 1/200, 1/250)$. The vertical dashed lines are located at $T = T_c$ (left) and at the “upturn” temperature scale (see text) $T = T_u$ (right).

which predicted a sharp increase of the drag resistivity as the temperature is lowered below the critical temperature of condensation.

In this Letter we show that the drag resistivity shows a precursor of the topological exciton condensed phase, *via* an upturn upon approaching the critical temperature, as shown in Fig. 1. Close to the critical temperature we find that on the basis of a Boltzmann analysis $\rho_D \propto \log(T - T_c)$. This upturn could therefore be used to determine the proximity to the phase transition. We note that the system considered here resembles double-layer graphene (DLG) – a system of two graphene layers

separated by a dielectric barrier. The main differences are the number of degenerate electron species and the dielectric constant [9, 10]. The results presented here are therefore also qualitatively applicable to DLG, a system for which exciton condensation has been predicted too [9, 11, 12]. Coulomb drag in DLG has been intensively studied theoretically [13]. This literature, however, refers to drag in which both layers are either electron- or hole-doped so that exciton condensation does not occur.

Coulomb drag and exciton condensation. — We consider a TI thin film whose top layer is electron-doped and whose bottom layer is hole-doped. We apply the “closed-band approximation” [9, 11, 12], *i.e.*, we consider only the upper Dirac cone for the electron layer and the lower Dirac cone for the hole layer. This is justified since the temperatures we consider are sufficiently small and the screening lengths sufficiently large, so that the far-lying bands can in first instance be considered inert. Then, the dispersions are well approximated by $\epsilon_t(\mathbf{k}) = v|\mathbf{k}| - \mu_t$ and $\epsilon_b(\mathbf{k}) = -v|\mathbf{k}| + \mu_b$ for the top and bottom layer, respectively ($\hbar = 1$ throughout this Letter). Here $v \approx 5 \times 10^5$ m/s is the Fermi velocity appropriate for the surface states of a typical TI thin film [14]. Note that the chemical potential for the electrons in the bottom layer is equal to $-\mu_b$. These formulas are valid up to a cutoff $\xi = 0.2$ eV, which is the typical distance between the Dirac point and the bulk bands in a TI. We also introduce the mean Fermi energy, $\mu = (\mu_t + \mu_b)/2$, and half the chemical potential imbalance, $h = (\mu_t - \mu_b)/2$.

Our theoretical treatment is based on the Boltzmann equation, whose main merit is to give a physically transparent picture of the scattering processes that control the momentum transfer rate between the layers. The crucial quantity in the Boltzmann approach is the scattering amplitude $V_{\text{eff}}(\mathbf{k}_1, \mathbf{k}_2, \mathbf{k}_3, \mathbf{k}_4)$, which is diagrammatically presented on the left-hand side in Fig. 2, where \mathbf{k}_1 and \mathbf{k}_2 are incoming electron momenta, one from each layer, and \mathbf{k}_3 and \mathbf{k}_4 outgoing electron momenta.

Under ordinary circumstances this interaction is well approximated by the single *screened* interaction line $V_0(|\mathbf{k}_1 - \mathbf{k}_4|, \epsilon_t(\mathbf{k}_1) - \epsilon_t(\mathbf{k}_4))$, which is shown as a wavy line in Fig. 2 (see Sect. I in Ref. [15]). But this simple picture breaks down in the vicinity of the exciton pairing transition, where it becomes necessary to include the effect of pairing fluctuations, diagrammatically represented by the infinite series of ladder diagrams shown in the right-hand side of Fig. 2. This series of diagrams diverges at the critical temperature T_c when the center-of-mass momentum of the electron-hole pair $\mathbf{K} = \mathbf{k}_1 - \mathbf{k}_3$ and the corresponding energy $\Omega = \epsilon_t(\mathbf{k}_1) - \epsilon_b(\mathbf{k}_3)$ tend to zero. Since the screened interlayer interaction V_0 is finite in the limit in which the momentum transfer $q = |\mathbf{k}_1 - \mathbf{k}_4|$ vanishes (*i.e.* it is not a long-range interaction), the qualitative behavior of the drag conductivity does not change

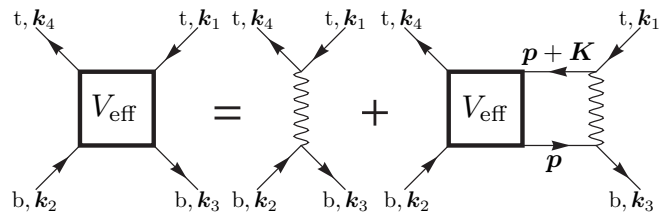


FIG. 2: The Bethe-Salpeter equation for the effective interaction V_{eff} in Eq. (1). The thin wavy line is V_0 and the arrows are the electron propagators in the top layer (top arrows) and the bottom layer (bottom arrows). Furthermore, $\mathbf{K} = \mathbf{k}_1 - \mathbf{k}_3 = \mathbf{k}_4 - \mathbf{k}_2$ is the center-of-mass momentum of the electron-hole pair and $\mathbf{q} = \mathbf{k}_1 - \mathbf{k}_4 = \mathbf{k}_3 - \mathbf{k}_2$ is the interlayer momentum transfer, which is responsible for Coulomb drag. Finally, \mathbf{p} is an integration variable. To make contact with the drag resistivity in Eq. (3) replace $\mathbf{k} = \mathbf{k}_1$ and $\mathbf{k}' = \mathbf{k}_2$.

when we neglect the momentum dependence of V_0 . In this case the ladder sum in Fig. 2 can be performed exactly. In this manner one obtains an effective interaction that depends only on the center-of-mass momentum \mathbf{K} and energy Ω as

$$V(\mathbf{k}_1, \mathbf{k}_2, \mathbf{k}_3, \mathbf{k}_4) \simeq V_{\text{eff}}(\mathbf{K}, \Omega) \equiv \frac{U}{1 - U\Xi(\mathbf{K}, \Omega)}, \quad (1)$$

where U is the momentum-independent contact interaction strength representing the screened interaction and

$$\Xi(\mathbf{K}, \Omega) = \frac{1}{A} \sum_{\mathbf{k}} \frac{n(\epsilon_t(\mathbf{k} + \mathbf{K})) - n(\epsilon_b(\mathbf{k}))}{\epsilon_b(\mathbf{k}) - \epsilon_t(\mathbf{k} + \mathbf{K}) - \Omega - i0^+} \quad (2)$$

is the pairing susceptibility, A being the 2D electron system area. The temperature T enters the above expression through the Fermi-Dirac distribution, $n(E) = 1/[1 + \exp(\beta E)]$, where $\beta = (k_B T)^{-1}$. It is easy to check that, in the symmetric case ($h = 0$) $\Xi(\mathbf{0}, 0)$ diverges logarithmically at zero temperature, and therefore the denominator of Eq. (1) must vanish at some non-zero temperature T_c no matter how small the electron-hole attraction. This is the mean-field pairing transition temperature. We see that, as the temperature is decreased towards T_c , pairing fluctuations first lead to an enhancement of V_{eff} for small \mathbf{K} and Ω and ultimately to a pole at $\Omega = 0$ and $\mathbf{K} = \mathbf{0}$ as $T = T_c$. The occurrence of this pole is the cause for the upturn of the Coulomb drag resistivity close to T_c .

By approximating V_0 by a contact interaction, we have introduced an unknown quantity in our theory, the contact interaction strength U , on which T_c depends. We stress that we do not calculate T_c by determining an estimate of U . Instead, we leave U as a parameter in our theory, the dependence on which we scale out in Fig. 1. We determine the actual value of T_c using an alternative calculation, which does take into account the dependence of V_0 on momentum (see Sect. II in Ref. [15]).

Inserting Eq. (1) in the Boltzmann collision integral and performing standard manipulations, we finally arrive at the following expression for the drag resistivity:

$$\begin{aligned} \rho_D = & -\frac{\beta}{2(2\pi)^6 e^2 n v^2} \int d\mathbf{K} d\Omega \frac{|V_{\text{eff}}(\mathbf{K}, \Omega)|^2}{\sinh^2(\beta\Omega/2)} \\ & \times \int d\mathbf{k} d\mathbf{k}' \Im m [b(\mathbf{k}; \mathbf{K}, \Omega)] \Im m [b(\mathbf{k}'; \mathbf{K}, \Omega)] \\ & \times [\mathbf{v}_t(\mathbf{k}' + \mathbf{K}) - \mathbf{v}_t(\mathbf{k} + \mathbf{K})] \cdot [\mathbf{v}_b(\mathbf{k}') - \mathbf{v}_b(\mathbf{k})], \quad (3) \end{aligned}$$

where $\mathbf{v}_{t(b)}(\mathbf{k}) \equiv \nabla \epsilon_{t(b)}(\mathbf{k})$ are the group velocities, n is the single layer carrier density, and

$$b(\mathbf{k}; \mathbf{K}, \Omega) \equiv \frac{n(\epsilon_t(\mathbf{k} + \mathbf{K})) - n(\epsilon_b(\mathbf{k}))}{\epsilon_b(\mathbf{k}) - \epsilon_t(\mathbf{k} + \mathbf{K}) - \Omega - i0^+} \quad (4)$$

is the summand of Eq. (2). Since $\mathbf{v}_t(\mathbf{k})$ and $\mathbf{v}_b(\mathbf{k})$ are oppositely directed ρ_D is positive, as expected for carriers of opposite polarities.

Drag Resistivity. — To determine the drag resistivity we need to evaluate Eq. (3) numerically. However, the qualitative behavior near T_c can be obtained analytically as follows (in what follows we first consider the balanced case $h = 0$). First, we notice that the denominator of Eq. (1) can be expanded, for small K and Ω as follows:

$$\begin{aligned} 1 - U\Xi(\mathbf{K}, \Omega) \simeq & \alpha(T) + a(T)U\nu_0(\beta v K)^2 \\ & + iU\nu_0\beta\Omega/4, \quad (5) \end{aligned}$$

where $\alpha(T) \propto T - T_c$ measures the distance from the critical point, $\nu_0 = \mu/(2\pi v^2)$ is the density-of-states at the Fermi energy, and $a(T)$ is a (dimensionless) positive ultraviolet-convergent quantity. Further, for $\mathbf{K} \rightarrow \mathbf{0}$ we have $[\mathbf{v}_t(\mathbf{k}' + \mathbf{K}) - \mathbf{v}_t(\mathbf{k} + \mathbf{K})] \cdot [\mathbf{v}_b(\mathbf{k}') - \mathbf{v}_b(\mathbf{k})] = 2v^2[\cos(\phi) - 1]$, where ϕ is the angle between \mathbf{k} and \mathbf{k}' . Since this quantity vanishes only in a set of zero measure with respect to the two 2D integrals over \mathbf{k} and \mathbf{k}' in Eq. (3), we can approximate the scalar product with a momentum-independent quantity of the order of v^2 . The integrals over \mathbf{k} and \mathbf{k}' can now be carried out analytically. Using that $\int d\mathbf{k} \Im m [b(\mathbf{k}; \mathbf{0}, \Omega)] = \Im m [\Xi(\mathbf{0}, \Omega)] = -\nu_0\beta\Omega/4$ for $\beta\Omega \ll 1$, we obtain

$$\begin{aligned} \rho_D \propto & \int d\mathbf{K} d\Omega \frac{(\beta\Omega/4)^2}{\sinh^2(\beta\Omega/2)} \\ & \times \frac{(\nu_0 U)^2 K}{[\alpha(T) + aU\nu_0(\beta v K)^2]^2 + (U\nu_0\beta\Omega/4)^2}, \quad (6) \end{aligned}$$

which is immediately seen to diverge logarithmically when $T \rightarrow T_c$, *i.e.*, for $\alpha \rightarrow 0$. This behavior is not altered by the momentum dependence of V_0 , since V_0 remains finite in the limit $q \rightarrow 0$ due to screening by carrier density fluctuations.

In Fig. 1 we show the numerically evaluated drag resistivity ρ_D as a function of temperature. We observe that for temperatures much larger than T_c , the drag resistivity increases quadratically as $\rho_D \propto T^2$ [16]. The

logarithmic divergence of $\rho_D \propto \log(T - T_c)$ is clearly visible. From top to bottom the curves correspond to $T_c/T_F = (1/150, 1/200, 1/250)$. Following Ref. [6], we define T_u as the temperature at which the upturn of ρ_D starts, as shown in Fig. 1. As a rule of thumb, $T_u \approx (3/2)T_c$.

Critical temperature. — In order to assess whether the upturn in the drag resistivity can be observed experimentally, we now need to actually calculate the (mean-field [17]) critical temperature as a function of interlayer distance and carrier density, taking into account screening effects [18]. To do so, we employ a separable approximation to the momentum-dependent interlayer interaction $V_0(|\mathbf{k}_1 - \mathbf{k}_4|, \epsilon_t(\mathbf{k}_1) - \epsilon_t(\mathbf{k}_4))$ — see Ref. [19] and Sect. II in Ref. [15]. The advantage of this approach over using a contact interaction is that it captures the decrease of the interaction strength V_0 with increasing transferred momenta. In particular, no ultraviolet cutoff on which the result for T_c would depend is needed.

As briefly explained in Sect. I of Ref. [15] and in much more detail in Ref. [20], the screened interlayer Coulomb interaction is given by $V_0(q, \omega) = V_{\text{tb}}(q)/\epsilon(q, \omega)$, where $V_{\text{tb}}(q)$ is the bare interaction between one electron on the top surface and one on the bottom surface, $q = |\mathbf{k} - \mathbf{k}'|$ and $\omega = \epsilon_b(\mathbf{k}) - \epsilon_b(\mathbf{k}')$ are momentum and energy transfers, respectively, and $\epsilon(q, \omega)$ is the dielectric screening function of the carriers, which we approximate in the random phase approximation. Both $V_{\text{tb}}(q)$ and $\epsilon(q, \omega)$ depend on the dielectric constants of the TI and of the environment surrounding the thin film.

We consider a TI film with vacuum above the top surface and a typical substrate material (*e.g.* SiO_2) below the bottom surface: the appropriate background dielectric constants are $\epsilon_{\text{top}} = 1$, $\epsilon_{\text{TI}} = 100$, $\epsilon_{\text{bottom}} = 4$. For the balanced case with $h = 0$ we obtain the phase diagram in Fig. 3. From right to left the lines correspond to carrier densities $n = (0.25, 0.5, 1) \times 10^{10} \text{ cm}^{-2}$. Our results show that the critical temperatures are within reach using existing cryogenic techniques for solid-state systems. Furthermore, also the required surface carrier densities have been reached previously [1]. In the inset of Fig. 3 we show the effect of a non-zero density imbalance. The solid curves represent the behavior of T_c/μ for constant $k_F d$. From top to bottom the curves correspond to $k_F d = (0.05, 0.075, 0.1)$. We note that T_c/μ decreases strongly with increasing density imbalance. The dashed line is the line along which the quartic term of the Ginzburg-Landau expansion of the free energy in powers of the order parameter, evaluated at T_c , vanishes (see Sect. III of Ref. [15]). Thus, for a fixed $k_F d$, the transition becomes first order as h grows beyond the intersection of the dashed line and the curve corresponding to that $k_F d$ value. The first-order region below the dashed line cannot be accurately described by our present normal-state formalism. The decreasing behavior of T_c with h indicates that the excitonic transition is strongly suppressed

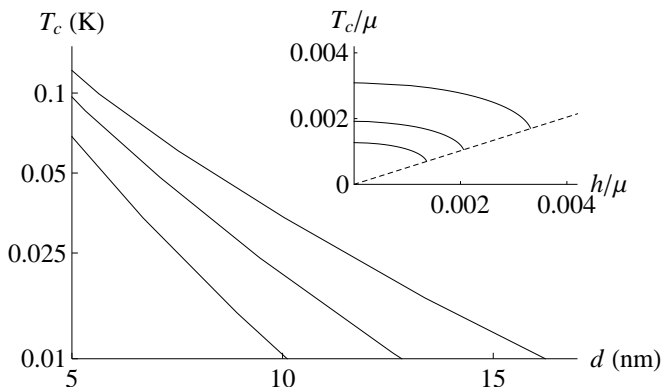


FIG. 3: Critical temperature T_c (in K) versus interlayer distance d (in nm) in the absence of density imbalance ($h = 0$). From right to left the lines correspond to carrier densities $n = (0.25, 0.5, 1) \times 10^{10} \text{ cm}^{-2}$. Inset: The critical lines T_c/μ versus h/μ . From top to bottom the lines correspond to $k_F d = (0.05, 0.075, 0.1)$. The critical lines terminate on the dashed line, *i.e.*, the locus of the points where the fourth order term of the Ginzburg-Landau expansion of the free energy in powers of the order parameter vanishes.

by the presence of any density imbalance. Thus, it is important in experimental realizations to have accurate control over the electron and hole densities in the two layers.

Discussion and conclusions. — Our theory predicts a divergence of ρ_D as T approaches T_c , but does not include the possible suppression of this divergence by critical fluctuations in the immediate vicinity of T_c . We expect that inclusion of these fluctuations leads to a down turn of ρ_D for temperatures very close to the critical temperature [21], before increasing again upon further decrease of the temperature, as predicted in Ref. [8].

We note that if the layers are brought too close together, the wave functions in the top layer and the bottom layer begin to overlap and interlayer tunneling becomes important. This limits our theory to a minimal interlayer distance $d \gtrsim 10$ nm. Actually, also conduction over the side layers of the TI film could be important. One expects that for samples of large enough area, these can be neglected. If not, a transport-prohibiting gap could be induced in the side layers by interfacing those with a ferromagnet.

In closing, we note that the upturn of ρ_D is analogous to the upturn of the spin-drag resistivity recently predicted in a cold gas of fermionic atoms near a ferromagnetic transition [22]. In particular, spin-fluctuation contributions to the effective interaction in the ferromagnetic case play the same role as pairing fluctuations in the present case. The reason why in Ref. [22] the spin drag resistivity was predicted to remain finite at T_c is that the transverse spin-fluctuation channel was treated

as part of the familiar (Hartree) charge and longitudinal spin-density fluctuation channels. When transverse spin fluctuations in the Fock channel are also included, a logarithmic divergence is obtained, just as in the present case. We also note that our results, while qualitatively similar to those obtained in Ref. [7] for massive electrons and holes in a conventional electron-hole semiconductor bilayer, differ, at the theoretical level, by the inclusion of an additional term in the collision integral. This term is easily missed by using the Kubo formula. The nature of the additional term is similar to the vertex corrections that are responsible for replacing the momentum lifetime by the transport lifetime in the classical Drude formula for the resistivity.

This work was supported by the Stichting voor Fundamenteel Onderzoek der Materie (FOM), the Netherlands Organization for Scientific Research (NWO), and by the European Research Council (ERC). G.V. was supported by the US Department of Energy grant DE-FG02-05ER46203. M.P. was supported by the Italian Ministry of Education, University, and Research (MIUR) through the program “FIRB - Futuro in Ricerca 2010” (project title “PLASMOGRAPH: plasmons and terahertz devices in graphene”).

* Electronic address: m.p.mink@uu.nl

- [1] M.Z. Hasan and C.L. Kane, Rev. Mod. Phys. **82**, 3045 (2010); X.-L. Qi and S.-C. Zhang, Rev. Mod. Phys. **83**, 1057 (2011).
- [2] B. Seradjeh, J.E. Moore, and M. Franz, Phys. Rev. Lett. **103**, 066402 (2009); see also Z. Wang *et al.*, arXiv:1106.5838.
- [3] T.J. Gramila *et al.*, Phys. Rev. Lett. **66**, 1216 (1991).
- [4] A.G. Rojo, J. Phys.: Condens. Matter **11**, R31 (1999).
- [5] A.F. Croxall *et al.*, Phys. Rev. Lett. **101**, 246801 (2008).
- [6] J.A. Seamons *et al.*, Phys. Rev. Lett. **102**, 026804 (2009).
- [7] Ben Yu-Kuang Hu, Phys. Rev. Lett. **85**, 820 (2000).
- [8] G. Vignale and A.H. MacDonald, Phys. Rev. Lett. **76**, 2786 (1996).
- [9] Yu. E. Lozovik and A.A. Sokolik, JETP Lett. **87**, **55** (2008).
- [10] S. Kim *et al.*, Phys. Rev. B **83**, 161401 (2011).
- [11] H. Min *et al.*, Phys. Rev. B **78**, 121401(R) (2008).
- [12] C.-H. Zhang and Y.N. Joglekar, Phys. Rev. B **77**, 233405 (2008).
- [13] W.-K. Tse, Ben Yu-Kuang Hu, and S. Das Sarma, Phys. Rev. B **76**, 081401(R) (2007); N.M.R. Peres, J.M.B. Lopes dos Santos, and A.H. Castro Neto, Europhys. Lett. **95**, 18001 (2011); M.I. Katsnelson, Phys. Rev. B **84**, 041407(R) (2011); E.H. Hwang and S. Das Sarma, arXiv:1105.3203v1.
- [14] See *e.g.* Y. Xia *et al.*, Nature Phys. **5**, 398 (2009).
- [15] Supplemental material file.
- [16] In the absence of pairing fluctuations, the dominant low-temperature behavior is $\rho_D \propto T^2 \log(T)$ and not $\rho_D \propto T^2$. The logarithmic correction is an artifact of the contact interaction used.

- [17] Berezinskii-Kosterlitz-Thouless (BKT) phase fluctuations tend to suppress T_c with respect to our mean-field estimate. The BKT temperature is given by $T_{\text{BKT}} = \pi\rho_s(T_{\text{BKT}})/2$, where $\rho_s(T)$ is the superfluid density, which can be estimated from a mean-field analysis. For DLG exciton condensates this analysis has been carefully carried out in Ref. [11].
- [18] M. Yu. Kharitonov and K.B. Efetov, Phys. Rev. B **78**, 241401 (2008); see also R. Bistritzer *et al.*, arXiv:0810.0331.
- [19] The T_c -equation is $1 = (1/A) \sum_{\mathbf{k}} V_{\text{sep}}^2(k) [n(\epsilon_t(\mathbf{k})) - n(\epsilon_b(\mathbf{k}))] / [\epsilon_b(\mathbf{k}) - \epsilon_t(\mathbf{k})]$, where $V_{\text{sep}}(k)$ is a separable approximation to the angular average of V_0 over incoming and outgoing momenta, *i.e.* $V_{\text{sep}}(k) = V_{\text{av}}(k, k_F) / \sqrt{V_{\text{av}}(k_F, k_F)}$ with $V_{\text{av}}(k, k') = \int d\phi V_0(q)|_{q=|\mathbf{k}-\mathbf{k}'|} [1 + \cos(\phi)] / (4\pi)$, where we have included the form factor $[1 + \cos(\phi)]/2$ relevant for this system [Yu. E. Lozovik and A.A. Sokolik, Eur. Phys. J. B **73**, 195 (2010); M.P. Mink *et al.*, Phys. Rev. B **84**, 155409 (2011)].
- [20] R.E.V. Profumo *et al.*, Phys. Rev. B **82**, 085443 (2010).
- [21] R. Kittinaradorn, R.A. Duine, and H.T.C. Stoof, arXiv:1107.2024.
- [22] R.A. Duine *et al.*, Phys. Rev. Lett. **104**, 220403 (2010).